



HAL
open science

Introducing clinical nanorachaeology: Isolation by co-culture of *Nanopusillus massiliensis* sp. nov.

Y. Hassani, J. Saad, E. Terrer, G. Aboudharam, B Giancarlo, F. Silvestri, D. Raoult, M. Drancourt, G. Grine

► To cite this version:

Y. Hassani, J. Saad, E. Terrer, G. Aboudharam, B Giancarlo, et al.. Introducing clinical nanorachaeology: Isolation by co-culture of *Nanopusillus massiliensis* sp. nov.. *Current Research in Microbial Sciences*, 2022, 3, pp.100100. 10.1016/j.crmicr.2021.100100 . hal-03590655

HAL Id: hal-03590655

<https://hal.science/hal-03590655>

Submitted on 8 Jan 2024

HAL is a multi-disciplinary open access archive for the deposit and dissemination of scientific research documents, whether they are published or not. The documents may come from teaching and research institutions in France or abroad, or from public or private research centers.

L'archive ouverte pluridisciplinaire **HAL**, est destinée au dépôt et à la diffusion de documents scientifiques de niveau recherche, publiés ou non, émanant des établissements d'enseignement et de recherche français ou étrangers, des laboratoires publics ou privés.



Distributed under a Creative Commons Attribution - NonCommercial 4.0 International License

Second revised version

1 **Introducing clinical nanorachaeology: Isolation by co-culture of *Nanopusillus***
2 ***massiliensis* sp. nov.**

3

4 Hassani Y. ^{1,2}, Saad J. ^{1,2}, Terrer E. ^{1,3}, Aboudharam G. ^{1,3}, Giancarlo B ⁴. Silvestri F. ³,
5 Raoult, D. ^{1,2}, Drancourt M. ^{1,2π}, Grine G. ^{1,3π*}

6

7 ¹ Aix-Marseille-Univ., IRD, MEPHI, IHU Méditerranée Infection, Marseille 13005,
8 France.

9 ² IHU Méditerranée Infection, Marseille 13005, France.

10 ³ Faculté de médecine dentaire, Aix-Marseille Université, Marseille 13005, France.

11 ⁴ Private practice Marseille France, Marseille, France.

12

13 π These two authors contributed equally to this work.

14 ***Corresponding author:** Ghiles GRINE, PhD

15 IHU Méditerranée Infection, 19-21 Boulevard Jean Moulin, 13005 Marseille, France.

16 **Phone :** (+33) 04 13 73 20 01 **Fax :** (+33) 4 13 73 24 02 ; **E-mail :**

17 grineghiles@gmail.com

18

19 Word count Abstract: **142**

20 Word count Text: **3190**

21

22

23 **ABSTRACT**

24 **Background**

25 Nanoarchaeota, obligate symbiont of some environmental archaea with reduced
26 genomes, have been described in marine thermal vent environments, yet never
27 detected in hosts, including humans.

28 **Methods**

29 Here, using laboratory tools geared towards the detection of nanoarchaea including
30 PCR-sequencing, WGS, microscopy and culture.

31 **Results**

32 We discovered a novel nanoarchaea, *Nanopusillus massiliensis*, detected in dental
33 plate samples by specific PCR-based assays. Combining fluorescent *in situ*
34 hybridization (FISH) with scanning electron microscopy disclosed close contacts
35 between *N. massiliensis* and the archaea *Methanobrevibacter oralis* in these samples.
36 Culturing one sample yielded co-isolation of *M. oralis* and *N. massiliensis* with a
37 606,935-bp genome, with 23.6% GC encoded 16 tRNA, 3 rRNA and 942 coding DNA
38 sequences, of which 400 were assigned to clusters of orthologous groups.

39 **Conclusion**

40 The discovery of *N. massiliensis*, made publicly available in collection, extended our
41 knowledge of human microbiota diversity, opening a new field of research in clinical
42 microbiology here referred to as clinical nanoarchaeology.

43

44 **Keywords:** *Nanopusillus massiliensis*, nanoarchaea, oral cavity

45 **Classification:** major categories

46

47 **INTRODUCTION**

48 Nanoarchaea are among the smallest known cellular organisms, exhibiting a 400-nm
49 diameter on average, hosting a small, hundreds of mega bases genome featuring an
50 extensive reduction in the number of protein and tRNA genes, resulting in massive loss
51 of biosynthetic capabilities, suggesting a parasitic-type of life¹⁻³. The first-ever detected
52 *Nanoarchaeum equitans* was accordingly co-cultured with hosting archaea *Ignicoccus*
53 *hospitalis* from deep-sea hydrothermal vents at the Kolbeinsey ridge, north of Iceland,
54 and several lines of microscopy observations demonstrated that both organisms were
55 tightly attached to each other⁴. The discovery of *N. equitans* opened a two-decade long
56 study of nanoarchaea in so-called extreme environments, and nanoarchaea have been
57 detected in extreme hot, acidophilic, and hypersaline environments and in temperate
58 lake and marine sediments⁵.

59 The search for nanoarchaea has been hampered by their extremely small size
60 and nonspecific cocci-like morphology, escaping routine microscopic observations,
61 while the unique structure of the 16S rRNA gene in nanoarchaea made them
62 undetectable by 16S rRNA gene detection^{6,7}. This situation has continued in clinical
63 microbiology laboratories, which are not archaea-oriented, up to the present work.
64 Indeed, our laboratory and a few others developed microscopy, nucleic acids-based and
65 culture methods targeted to the detection of archaea in clinical samples representative
66 of physiological microbiota, notably those in the oral cavity and gut⁸⁻¹⁰ and of
67 pathological dysbiosis¹¹⁻¹⁵, abscesses and more recently archaeamia¹⁶⁻¹⁸.

68 In this report, after having developed laboratory tools geared towards the specific
69 detection of nanoarchaea in clinical samples, we report the unprecedented observation

70 of nanoarchaea in the human oral cavity microbiota, culminating with the whole genome
71 sequence-based discovery of the novel *Nanopusillus massiliensis*.

72 **MATERIALS AND METHODS**

73 **Sample collection.** This study included a series of dental plaque samples collected
74 between December 2019 and August 2020 from patients in the Odontology Department,
75 Timone Hospital, Marseille. Dental plaque samples, considered waste, usually
76 aspirated, and discarded, were collected through the suction cannulas. All patients
77 received information about the study and gave informed consent prior to the
78 investigation. Accordingly, dental plates were collected anonymously using a sterile
79 Gracey dental curette (Hu-Friedy, Rotterdam, Netherlands) or a sterile micro brush. All
80 samples were immediately placed into a Hungate tube (Dominique Dutscher, Brumath,
81 France) containing 5 mL of a specific transport SAB medium previously described¹⁹.

82 **PCR-based detection of nanoarchaea.** Examining the pangenome of 345 archaea
83 and two nanoarchaea *N. equitans*²⁰ (GenBank accession number AE017199.1) and
84 *Candidatus N. acidilobi*²¹ (GenBank accession number CP010514.1) using the Roary
85 pan-genome pipeline in Galaxy software (<https://usegalaxy.org.au/>) (**SI Appendix, Fig.**
86 **S1**), we determined that the 30S SSU L12 gene conserved among these 347 organisms
87 exhibited a species-specific sequence. More specifically, the 873-bp nanoarchaea 30S
88 SSU L12 gene exhibited sequence similarity < 95% with homologous sequences in
89 methanogenic archaea (here designed as methanogens). A PCR primer pair (forward
90 primer: 5'-TGAAAGCAAAGGGATTTTATTCA-3'; reverse primer 5'-
91 TTGCATGTGGAACAATACCAG-3') (Eurogentec, Seraing, Belgium) was designed
92 using Primer-Blast (<https://www.ncbi.nlm.nih.gov/tools/primer-blast/>) to specifically

93 amplify a 188-bp fragment of the nanoarchaea 30S SSU L12 gene and specify
94 nanoarchaea species, by sequencing. PCR primers were incorporated into a 50 µL-
95 volume containing 25 µL Amplitaq Gold ® (Thermo Fisher Scientific, Illkirch-
96 Graffenstaden, France), 2 µL each primer (10 pM), 16 µL Dnase/Rnase-free distilled
97 water (Gibco, Cergy-Pontoise, France) and 5 µL of extracted DNA. DNA was extracted
98 on dental plates using 15-minute sonication followed by automatic extraction using the
99 EZ1 Advanced extraction kit (QIAGEN, Hilden, Germany) as previously described¹⁸.
100 The reaction mixture was then subjected to a 40-cycle PCR program comprising a 30-
101 second denaturation step at 95° C, followed by 45-second hybridization at 60° C and 1-
102 minute elongation at 72° C. Each amplification program started with denaturation at 95°
103 C for 15 minutes and ended with a final elongation step at 72° C for 5 minutes. Non-
104 inoculated transport medium was used as a negative control. PCR products were
105 sequenced as previously described²². In parallel, samples along with negative controls
106 were assayed for the presence of methanogens by PCR-sequencing targeting the broad
107 range archaeal 16S rRNA gene SDArch0333aS15, 5-TCCAGGCCCTACGGG-3 and
108 SDArch0958aA19, 5-YCCGGCGTTGAMTCCAATT-3)¹⁵. PCR products were
109 sequenced using the same primers as used for PCRs, as previously reported²².

110 **Microscopic observations of nanoarchaea.** Nanoarchaea PCR-positive clinical
111 samples were examined by microscopy with and without sample deglycosylation aimed
112 at degrading biofilms and facilitating further microscopic observations. As for
113 deglycosylation, 140 µL of sample were incubated for one hour with 20 µL Endo Hf
114 (New England Biolabs, Evry-Courcouronnes, France) at 37° C. As for scanning electron
115 microscopy, 100 µL of 2.5% glutaraldehyde-fixed sample were cytocentrifuged onto a

116 glass slide (Shandon cytospin, Thermo Scientific, Waltham, MA, USA), stained for 2
117 minutes by 1% phosphotungstic acid (Sigma Aldrich, Saint-Louis, MO, USA) at room
118 temperature and observed using a TM4000 Plus scanning electron microscope (Hitachi,
119 Tokyo, Japan). Also, fluorescent *in situ* hybridization (FISH) incorporated the archaea-
120 specific Arch915 probe Alexa 647 (5'-GTGCTCCCCCGCCAATTCCT-3') and the
121 nanoarchaeota 16S rRNA gene probe 515mcR2 probe Alexa488 (5'-
122 CCCTCTGGCCCACTGCT-3'), as previously described²¹.

123 **Nanoarchaea genome analyses.** Total DNA extracted from one nanoarchaea PCR
124 positive sample was sequenced three times on the MiSeq platform (Illumina Inc, San
125 Diego, CA, USA) using the Nexera XT DNA sample prep kit (Illumina), with the paired
126 end strategy. The tagmentation step fragmented and tagged each extracted DNA to
127 prepare the paired-end library. A limited PCR amplification (12 cycles) was then
128 performed to complete the tag adapters and to introduce dual-index barcodes. DNA was
129 then purified on AMPure XP beads (Beckman Coulter Inc, Fullerton, CA, USA). In
130 addition, according to the Nextera XT protocol (Illumina), all libraries were normalised
131 on specific beads. We then pooled all libraries into one library for DNA sequencing on
132 MiSeq. The pooled single strand library was loaded onto the reagent cartridge and then
133 onto the instrument along with the flow cell. Automated cluster generation and paired
134 end sequencing with dual index reads were performed in a single 39-hour run in 2 x
135 250-bp. For each sample/purified nanoarchaea DNA sequence, the quality of each
136 Illumina read was checked by FastQC and trimmed using trimmomatic version 0.36.6.
137 Sequence reads were concatenated and assembled using SPAdes version 3.5.0
138 software²³. Finishing was achieved by LongRange PCR (LR-PCR) followed by next-

139 generation sequencing after PCR primers were designed by aligning nanoarchaea on-
140 going genome sequence with *Candidatus N. acidilobi* reference genome, targeting
141 regions to be finished (**SI Appendix, Table S5**). Purified LR-PCR products were
142 sequenced using the Illumina Iseq technique as previously described²⁴. Contigs were
143 identified using Blastn against NCBI database and concatenated reads were mapped
144 using CLCgenomic version 7 against the *Candidatus N. acidilobi* genome sequence.
145 The nanoarchaea genome, annotated using Prokka software²⁵, was added to a
146 nanoarchaea pangenome analysis performed using Roary pan-genome pipeline, as
147 above. Genomic similarity of the on-going nanoarchaea with closely related species was
148 estimated using the OrthoANI software²⁶ and digital DNA-DNA hybridization (dDDH)
149 performed using Type (Strain) Genome Server (TYGS) (<https://tygs.dsmz.de/>)²⁷. The
150 new nanoarchaea genome was then incorporated into a rhizome representation, using a
151 previously described protocol²⁸. Putative encoded protein functions were searched
152 against the Clusters of Orthologous Groups (COG) database using BLASTP (E-value
153 1e-03, coverage 0.7 and identity percent 30%). Secretion systems were searched via
154 the MacSyDB/TXSSdb database. Further metabolic pathway repertory was established
155 with a RAST server. Lastly, *in silico* antibiotic resistance profiling of *N. massiliensis* was
156 determined according to Abricate, Resfinder, Card and Argannot databases with a
157 minimum of 10% identity.

158 **Co-culturing nanoarchaea.** A dental plaque sample positive for methanogens and
159 nanoarchaea by PCR-sequencing was collected in a Hungate tube (Dominique
160 Dutscher) containing 3 mL of transport SAB medium¹⁹. As for inoculation, a culture
161 bottle was prepared under a strict anaerobic atmosphere in a BACT/ALERT® blood

162 culture bottle (bioMérieux, Craaponne, France) emptied of its original broth and
163 atmosphere, replaced by 30 mL of SAB medium¹⁹ used as an antibiotic-free enrichment
164 medium under an 80% H₂-20% CO₂ atmosphere. Then, one milliliter of inoculated SAB
165 transport medium was inoculated into the conditioned bottle, incubated for 15 days in a
166 Virtuo apparatus (bioMérieux) at 37° C under constant shaking. After 15-day incubation,
167 CH₄ production was detected in the positive polarity using helium as reference gas in a
168 Clarus 580 gas chromatograph (Perkin Elmer, Villebon-sur-Yvette, France). After
169 methane was detected, 17 mL of broth were ultracentrifuged at 25,000 g for two hours
170 at 4° C using SORVALL Discovery 90SE with Surespin 630 rotor (Kendro Laboratory
171 Product, Burladingen, Germany). The pellet was observed by scanning electron
172 microscopy and FISH in the presence of a pure culture of *M. oralis* strain VD9²⁹
173 (demonstrated to be nanoarchaea-free by PCR) used as a nanoarchaea negative
174 control, using methods above described. After observation of pelleted methanogens and
175 nanoarchaea, the pellet was deglycosylated as described above prior to its inoculation
176 in SAB medium supplemented with a vitamin cocktail (Sigma Aldrich, Merck) (**SI**
177 **Appendix, Table S2**), 0.1g D-fructose (Sigma Aldrich), a fatty acid mixture (1 mL of a
178 solution of isobutyric acid, 2-methylbutyric acid, isovaleric acid and valeric acid) (Sigma
179 Aldrich) and 5% of 0.22 µm-filtered bovine rumen. Transport medium inoculated with
180 phosphate-buffered saline was incorporated as a negative control. Co-culture was
181 metagenome-sequenced by using a home-adapted NovaSeq protocol (Illumina Inc.) (**SI**
182 **Appendix, 1**) In parallel in the perspective of methanogen isolation, 200 µL of 15-day
183 incubation broth culture were inoculated onto SAB solid medium as previously
184 described¹⁹.

185 **RESULTS**

186 **Molecular detection of *N. massiliensis*.** A total of 102 samples collected from 102
187 patients were investigated for the presence of methanogens and nanoarchaea by using
188 specifically designed archaeal (16S rRNA gene) and nanoarchaea (30S L12 gene)
189 gene-based PCR systems, as described below. While all the negative controls
190 introduced in every batch of PCR remained negative, 22 (21.6%) methanogen 16S
191 rRNA gene amplicons were detected dental plate samples. Sequencing indicated that
192 the 15/22 dental plaque amplicons exhibited 99% sequence similarity with reference
193 16S rRNA gene sequence of *M. oralis* strain VD9 (accession NCBI: LN898260.1); 2
194 dental plaque amplicons exhibited 99.8% sequence similarity with the reference 16S
195 rRNA gene sequence of *M. oralis* strain M2 CSUR P5920 (accession NCBI:
196 LR590665.1); and 5 dental plaque amplicons exhibited 99% sequence similarity with the
197 reference 16S rRNA gene sequence of *Methanobrevibacter massiliensis* N58C
198 (accession NCBI: LN610763.1). Further, in the negativity observed in the negative
199 controls, nanoarchaea were PCR-detected in 5 (4.90%) dental plate samples collected
200 from 5 different patients. Sequencing indicated that these 5 amplicons exhibited 95.7%
201 sequence similarity and 100% cover with the homologous 30S L12 gene sequence of
202 *Candidatus Nanopusillus acidilobi* (accession NCBI CP010514.1), indicative of a novel
203 nanoarchaea, here reported as *Nanopusillus massiliensis* sp. nov., co-detected with *M.*
204 *oralis* in 4 dental plate samples and with *M. massiliense* in 1 dental plate sample.

205 **Microscopic observation of *N. massiliensis*.** FISH detected nanoarchaea-forming
206 cocci attached to the surface of a methanogen, for which bacillary morphology
207 suggested *M. oralis*, in 4 nanoarchaea PCR-positive dental plates (**Fig. 1A and 1B**).

208 Further scanning electron microscopy of these 4 samples showed 300-500 nm diameter
209 cells attached to the surface of *M. oralis* cells, exhibiting a characteristic diameter of <
210 0.7-1.2 μm and elongated morphology³⁰ (**Fig. 1C and 1D**), whereas such small cells
211 were not observed in the negative controls (**SI Appendix, Fig. S2**).

212 ***N. massiliensis* genome features.** After three runs of MiSeq sequencing, a dental
213 plaque sample PCR-positive for nanoarchaea and *M. oralis* yielded 3,125,000 paired
214 end reads and the generated read length is between 1 and 3000bp, which were
215 assembled and blasted against the nr database. After 12 *Methanobrevibacter* sp.
216 contigs were detected, remaining reads were mapped against the *Candidatus N.*
217 *acidilobi* reference genome using 0.5 length fraction and 0.3 similarity fraction as
218 mapping parameters, to recover a 606,947-bp unique contig exhibiting a gap ratio of
219 19%, with N-bearing regions varying from two bp to 1,200-pb, representative of a draft
220 genomic sequence of *N. massiliensis*. Finishing yielded a unique 606,947-bp long
221 chromosome sequence (WGS accession number: CAKLBW000000000; 16S rRNA
222 gene sequencing accession: Q6268) with 23.6% GC encoding 16 tRNA, 3 rRNA and
223 942 coding DNA sequences, of which 400 were assigned to clusters of orthologous
224 groups (COGs) (**SI Appendix, Table S3**). A nine-nanoarchaea pangenome, including
225 *N. massiliensis*, incorporated 5,294 genes, including 4,329 cloud genes and 959 shell
226 genes. Six genes were common to the 9 nanoarchaea genomes; they encoded the 50S
227 ribosomal protein L18, 50S ribosomal protein L23, 30S ribosomal protein S19, 30S
228 ribosomal protein S5, DNA-directed RNA polymerase subunit K and replication factor C
229 small subunit (**SI Appendix, Fig. S3**). We observed that single nucleotide
230 polymorphisms (SNPs) varied from 29 SNPs between the novel nanoarchaea and

231 *Candidatus N. acidilobi* up to 615 SNPs between *N. massiliensis* and Nanoarchaeota
232 archaeon isolate B33_G15 (**SI Appendix, Fig. S4 and Table S4**). The maximum
233 OrthoANI value was 95.21% between new nanoarchaea *N. massiliensis* and
234 *Candidatus N. acidilobi* (**SI Appendix, Fig. S6**), which exhibited a maximum dDDH
235 value of 69.4 (confidence interval = [66.4 - 72.2]) (**SI Appendix Table S5**). A mosaic
236 representation of rhizome incorporating 1,457 genes indicated that 618 (42.4%) novel
237 nanoarchaea genes overlapped with DPANN-nanoarchaea, 191 (13.1%) with other
238 members of the DPANN superphylum (Diapherotrites, Parvarchaeota,
239 Aenigmarchaeota, Nanoarchaeota and Nanohaloarchaeota, Micrarchaeota,
240 Woesarchaeota), 399 (27.38 %) with Archaea, 69 (4.73 %) with Bacteria, 12 (0.82 %) with Candidate phyla radiation, 10 (0.68%) with virus, 3 with Asgard and 3 with
242 Eukaryota, whereas 157 (10.57%) genes were orphans (**Fig. 1F**). Furthermore, no
243 antibiotic resistance determinant was detected, nor were any secretion systems
244 identified.

245 ***N. massiliensis* metabolism.** A Venn diagram incorporating enzymes detected by
246 RAST annotation in *N. massiliensis*, *Candidatus N. acidilobi* and *M. oralis* genomes
247 detected five enzymes unique to *N. massiliensis*: i.e., lead, cadmium, zinc and mercury
248 transporting ATPase, copper-translocating P-type ATPase, DNA reverse gyrase,
249 alkaline phosphatase and cell division protein FtsH. A total of 108 enzymes were unique
250 to *M. oralis* and 14 enzymes were common to *M. oralis*, *Candidatus N. acidilobi* and *N.*
251 *massiliensis* (**SI Appendix, Fig. S5 and Table S6**). The *N. massiliensis* genome
252 encoded seven enzymes participating in glycolysis. Likewise, the *N. massiliensis*
253 genome encoded five gluconeogenesis enzymes and enzymes involved in the complete

254 synthesis and degradation of glycogen. RAST annotation showed that *N. massiliensis*
255 was not able to synthesize purines and pyrimidines, nor had any alternative metabolism
256 to obtain the nucleoside monophosphates, diphosphates and triphosphates for the
257 synthesis of nucleic acids. Instead, we detected ribonucleoside-diphosphate reductase
258 subunit alpha (providing necessary precursors for DNA synthesis), catalyzing the
259 biosynthesis of deoxyribonucleotides from the corresponding ribonucleotides. Similarly,
260 *N. massiliensis* was not found to be able to synthesize amino acids, whereas 19
261 aminoacyl-tRNA biosynthesis genes were detected. *N. massiliensis* had the potential to
262 catabolize inorganic sulfur compounds: we detected sulfate adenylyltransferase that
263 may catalyze the formation of adenosine 5'-phosphosulfate from ATP and inorganic
264 sulfate. As described for other nanoarchaea, *N. massiliensis* lacked a membrane ATP
265 synthase complex as well as all components participating in the respiratory chain, but
266 encoding a reduced repertoire of transporters, including two ATP-binding cassette
267 (ABC) transporters and a Major facilitator superfamily (MFS) transporter. We detected
268 only one protein (FlaL) of the archaellum complex (archaeal flagellum), leaving
269 unknown whether *N. massiliensis* has motility (**Fig. 2**).

270 ***N. massiliensis* isolation by co-culture.** After PCR-sequencing co-detected *N.*
271 *massiliensis* with *M. oralis*, suggesting that *M. oralis* could host *N. massiliensis*, we used
272 an enrichment medium promoting *M. oralis* growth and, consequently, growth of *M.*
273 *oralis*-associated nanoarchaea to inoculate one dental plaque sample. After methane
274 was detected at day 15, PCR-sequencing targeting 30S was positive on both
275 supernatant and pellet issuing from this culture. However, only the pellet, but not the
276 supernatant, yielded cocci-like nanoarchaea sized 200-400 nm, either as free cells or

277 located around *M. oralis* cells, as observed by scanning electron microscopy in parallel
278 to fluorescent *in situ* hybridization, the observations being enhanced by deglycosylation
279 of the pellet (**Fig. 3**). In parallel, colonies of hosting *M. oralis* observed at day 10 were
280 firmly identified as *M. oralis* (strain YH) by PCR-sequencing of the 16S rRNA gene (The
281 16S rRNA gene sequence accession is OU484279, the GenBank access number of
282 genome is CAJVUI000000000), exhibiting 100% sequence similarity with the
283 homologous 16S rRNA gene sequence of *M. oralis* strain VD9 (accession NCBI:
284 LN898260.1). *M. oralis* strain YH colonies were sub-cultured on liquid SAB medium,
285 and viability and culture of the strain were monitored by CH₄ detection, as described
286 above. *M. oralis* strain YH whole genome sequence (1.9 Mp) yielded a DDH value of
287 97% with reference *M. oralis* strain M2 CSUR P5920, firmly confirming the identity of
288 strain YH, which has been made available by depository in the Collection de Souches
289 de l'Unité des Rickettsies (CSUR, WDCM875) as CSUR Q6267, while the co-culture *M.*
290 *oralis*-*N. massiliensis* has been deposited under number CSUR Q6268.

291

292 **Description of the novel species *Nanopusillus massiliensis* sp.nov.**

293 We report co-culture isolation of *Nanopusillus massiliensis* as the first co-isolated
294 member of Nanoarchaeota of human origin, a strain representative of a new species in
295 the previously described genus *Nanopusillus* within the phylum Nanoarchaeota. Its
296 formal description is provided below.

297

298 *Nanopusillus massiliensis* sp. nov.

299 Etymology. Nanus (Latin adj.) 'dwarf', referring to its size and denoting placement in the

300 Nanoarchaeota; pu'sil.lus (Latin adj.) very small, indicating its extremely small size, at
301 the limit of cellular life, like its closest neighbour *Nanopusillus acidilobi*; mas.si.li.en'sis.
302 L. fem. adj. massiliensis referring to Massilia, the past Roman name of Marseille,
303 France where this nano-organism has been discovered.
304 Coccoid cells, 150-400 nm in diameter, obligate ectosymbionts/parasites on the surface
305 of the methanogen *Methanobrevibacter oralis*. Occasional free cells may be observed in
306 the co-culture, which viability is unknown. Optimal growth occurs in co-culture with its
307 host at 37°C and pH 7. Initially isolated from human dental plaque. *N. massiliensis* has
308 been deposited in the Collection de Souches de l'Unité des Rickettsies (CSUR) under
309 CSUR Q6268.

310

311 **DISCUSSION**

312 We here report the unprecedented observation of nanoarchaea in clinical specimens,
313 authenticated by concurring results obtained in the very same clinical samples by
314 unrelated laboratory methods consisting of microscopic observations, molecular
315 investigations culminating in one whole genome sequence and isolation in co-culture in
316 the presence of negative controls introduced in every experimental step; for a group of
317 nano-organisms that had never been previously studied in our laboratory.

318 This discovery was made possible after we developed nanoarchaea-oriented
319 specific laboratory tools, capitalizing on the previous expertise that we have acquired
320 over years in the clinical microbiology of archaea, methanogens and halophilic
321 archaea³¹, including their potential role in pathological situations in dysbiosis⁹, anaerobe
322 abscesses^{16,17,32} and archaeamia¹⁸. Routinely available scanning electron microscopy
323 was highly contributive to this work and discovery. Nevertheless, nanoarchaea specific

324 molecular detection tools and isolation by culture detailed in this report can be
325 translated to any clinical microbiology laboratory with expertise in the manipulation of
326 oxygen-intolerant microorganisms, to set-up the prospective search for nanoarchaea in
327 microbiota and pathological samples.

328 The novel nanoarchaea *N. massiliensis* was co-detected by microscopy,
329 molecular techniques and co-isolation and culture with hosting methanogen *M. oralis*.
330 Several lines of microscopy observations indicated that *N. massiliensis* tightly attaches
331 to *M. oralis*, an observation previously reported for the environmental *N. equitans*
332 attaching to hosting *I. hospitalis*³³. In the latter example, electron cryotomography
333 disclosed either direct contacts between the two organism membranes, as we observed
334 here, or fibrous material bridging the two organisms, an observation that we did not
335 make here, despite *N. massiliensis* encoding one flagellum component similar to
336 secretion type IV, previously reported to sustain physical relationships between another
337 group of nano-organisms, the *Candidate phyla radiation* and host bacteria³⁴.

338 Nevertheless, tight connections between *M. oralis* and *N. massiliensis* may favor
339 metabolite exchanges through ABC transporters, of which two representative families
340 are encoded by the *N. massiliensis* genome. In the absence of a complete glycolysis
341 pathway, *N. massiliensis* energy production may rely on gluconeogenesis and ABC
342 transporter importation of fructose, metabolized into fructose 6-phosphate. Likewise, the
343 inability of *N. massiliensis* to synthesize purines and pyrimidines could be overcome by
344 a ribonucleoside diphosphate reductase providing precursors for DNA synthesis,
345 catalyzing deoxyribonucleotide biosynthesis from the corresponding ribonucleotides.
346 The inability to synthesize amino acids may be overcome by their recovery resulting

347 from extracellular protein degradations, in line with detection of 19 aminoacyl t-RNA in
348 the *N. massiliensis* genome. Finally, detection of sulfate adenylyl-transferase suggested
349 that *N. massiliensis* incorporated organic sulfur into organic molecules involved in
350 cofactors and amino acids synthesis, gaining an advantage for its habitat in the oral
351 cavity hosting sulfate-reducing bacteria³⁵.

352 *N. massiliensis* is the only human-cultured nanoarchaea, strikingly broadening
353 the spectrum of ecological niches when searching for intriguing nanoorganisms.
354 Previously the only known representatives *N. equitans*, *Candidatus N. acidilobi*,
355 *Candidatus Nanobsidianus stetteri* and *Candidatus Nanoclepta minutus* have been
356 detected in so-called extreme environmental ecosystems² featuring thermophilic
357 organisms growing at about 80° C, and organisms also growing in acidic environments
358 at pH 6 and a salinity concentration of 2%²¹. However, nanoarchaeales sequences have
359 also been identified in ecosystems with temperatures ranging from 4° C to 10° C and 6°
360 C to 67° C³⁶.

361 The discovery of the novel nanoarchaea *N. massiliensis* is opening a completely
362 new field of clinical investigations that we have named clinical nanoarchaeology,
363 consisting of establishing the repertoire of nanoarchaea in various human microbiota
364 along with specifying their role in the physiology of those microbiota; and we detail in
365 this report some laboratory keys to access this new world in clinical microbiology.

366

367 **REFERENCES**

- 368 1. Casanueva, A., Tuffin, M. & Cowan, D. A. 1 The Nanoarchaeota: Physiology,
369 Genomics and Phylogeny, *Archaea: Structure, Habitats and Ecological Significance*
370 Chapters. NOVA sciences publishers, 163-174 (2011).
- 371 2. John, E. S., Flores, G. E., Meneghin, J. & Reysenbach, A.-L. Deep-sea
372 hydrothermal vent metagenome-assembled genomes provide insight into the
373 phylum Nanoarchaeota. *Environ. Microbiol. Rep.* **11**, 262–270 (2019).
- 374 3. Nakai, R. Size Matters: Ultra-small and Filterable Microorganisms in the
375 Environment. *Microbes Environ.* **35**, (2020).
- 376 4. Huber, H. *et al.* A new phylum of Archaea represented by a nanosized
377 hyperthermophilic symbiont. *Nature* **417**, 63–67 (2002).
- 378 5. Castelle, C. J. & Banfield, J. F. Major New Microbial Groups Expand Diversity and
379 Alter our Understanding of the Tree of Life. *Cell* **172**, 1181–1197 (2018).
- 380 6. Casanueva, A. *et al.* Nanoarchaeal 16S rRNA gene sequences are widely dispersed
381 in hyperthermophilic and mesophilic halophilic environments. *Extremophiles* **12**,
382 651–656 (2008).
- 383 7. Baker, G. C., Smith, J. J. & Cowan, D. A. Review and re-analysis of domain-specific
384 16S primers. *J. Microbiol. Methods* **55**, 541–555 (2003).
- 385 8. Nguyen-Hieu, T., Khelaifia, S., Aboudharam, G. & Drancourt, M. Methanogenic
386 archaea in subgingival sites: a review. *APMIS* **121**, 467–477 (2013).
- 387 9. Grine, G. *et al.* Tobacco-smoking-related prevalence of methanogens in the oral
388 fluid microbiota. *Sci. Rep.* **8**, 9197 (2018).
- 389 10. Nkamga, V. D., Henrissat, B. & Drancourt, M. Archaea: Essential inhabitants of the
390 human digestive microbiota. *Hum. Microbiome J.* **3**, 1–8 (2017).

- 391 11. Huynh, H. T. T., Pignoly, M., Drancourt, M. & Aboudharam, G. A new methanogen
392 “*Methanobrevibacter massiliense*” isolated in a case of severe periodontitis. *BMC*
393 *Res. Notes* **10**, 657 (2017).
- 394 12. Belkacemi, S. *et al.* Peri-implantitis-associated methanogens: a preliminary report.
395 *Sci. Rep.* **8**, 9447 (2018).
- 396 13. Scanlan, P. D., Shanahan, F. & Marchesi, J. R. Human methanogen diversity and
397 incidence in healthy and diseased colonic groups using *mcrA* gene analysis. *BMC*
398 *Microbiol.* **8**, 79 (2008).
- 399 14. Million, M. *et al.* Increased Gut Redox and Depletion of Anaerobic and
400 Methanogenic Prokaryotes in Severe Acute Malnutrition. *Sci. Rep.* **6**, 26051 (2016).
- 401 15. Grine, G. *et al.* Detection of *Methanobrevibacter smithii* in vaginal samples collected
402 from women diagnosed with bacterial vaginosis. *Eur. J. Clin. Microbiol. Infect. Dis.*
403 **38**, 1643–1649 (2019).
- 404 16. Nkamga, V. D. *et al.* *Methanobrevibacter oralis* detected along with *Aggregatibacter*
405 *actinomycetemcomitans* in a series of community-acquired brain abscesses. *Clin.*
406 *Microbiol. Infect. Off. Publ. Eur. Soc. Clin. Microbiol. Infect. Dis.* **24**, 207–208 (2018).
- 407 17. Nkamga, V. D., Lotte, R., Roger, P.-M., Drancourt, M. & Ruimy, R.
408 *Methanobrevibacter smithii* and *Bacteroides thetaiotaomicron* cultivated from a
409 chronic paravertebral muscle abscess. *Clin. Microbiol. Infect. Off. Publ. Eur. Soc.*
410 *Clin. Microbiol. Infect. Dis.* **22**, 1008–1009 (2016).
- 411 18. Drancourt, M. *et al.* *Methanobrevibacter smithii* Archaemia in Febrile Patients with
412 Bacteremia, Including Those with Endocarditis. *Clin. Infect. Dis.* (2020)
413 doi:10.1093/cid/ciaa998.

- 414 19. Khelaifia, S., Raoult, D. & Drancourt, M. A Versatile Medium for Cultivating
415 Methanogenic Archaea. *PLOS ONE* **8**, e61563 (2013).
- 416 20. Waters, E. *et al.* The genome of *Nanoarchaeum equitans*: Insights into early
417 archaeal evolution and derived parasitism. *Proc. Natl. Acad. Sci.* **100**, 12984–12988
418 (2003).
- 419 21. Wurch, L. *et al.* Genomics-informed isolation and characterization of a symbiotic
420 Nanoarchaeota system from a terrestrial geothermal environment. *Nat. Commun.* **7**,
421 12115 (2016).
- 422 22. Dridi, B., Henry, M., Khéchine, A. E., Raoult, D. & Drancourt, M. High Prevalence of
423 *Methanobrevibacter smithii* and *Methanosphaera stadtmanae* Detected in the
424 Human Gut Using an Improved DNA Detection Protocol. *PLOS ONE* **4**, e7063
425 (2009).
- 426 23. Bankevich, A. *et al.* SPAdes: A New Genome Assembly Algorithm and Its
427 Applications to Single-Cell Sequencing. *J. Comput. Biol.* **19**, 455–477 (2012).
- 428 24. Tulloch, R. L., Kok, J., Carter, I., Dwyer, D. E. & Eden, J.-S. An Amplicon-Based
429 Approach for the Whole-Genome Sequencing of Human Metapneumovirus. *Viruses*
430 **13**, 499 (2021).
- 431 25. Seemann, T. Prokka: rapid prokaryotic genome annotation. *Bioinformatics* **30**,
432 2068–2069 (2014).
- 433 26. OrthoANI: An improved algorithm and software for calculating average nucleotide
434 identity | Microbiology Society.
435 <https://www.microbiologyresearch.org/content/journal/ijsem/10.1099/ijsem.0.00076>
436 crawler=true.

- 437 27. Meier-Kolthoff, J. P., Klenk, H.-P. & Göker, M. 2014. Taxonomic use of DNA G+C
438 content and DNA–DNA hybridization in the genomic age. *Int. J. Syst. Evol.*
439 *Microbiol.* **64**, 352–356.
- 440 28. Togo, A. H. *et al.* Culture of Methanogenic Archaea from Human Colostrum and
441 Milk. *Sci. Rep.* **9**, 18653 (2019).
- 442 29. *Methanobrevibacter oralis* partial 16S rRNA gene, strain VD9. (2015).
- 443 30. Ferrari, A., Brusa, T., Rutili, A., Canzi, E. & Biavati, B. Isolation and characterization
444 of *Methanobrevibacter oralis* sp. nov. *Curr. Microbiol.* **29**, 7–12 (1994).
- 445 31. Khelaifia, S. *et al.* Genome sequence and description of *Haloferax massiliense* sp.
446 nov., a new halophilic archaeon isolated from the human gut. *Extremophiles* **22**,
447 485–498 (2018).
- 448 32. Drancourt, M. *et al.* Evidence of Archaeal Methanogens in Brain Abscess. *Clin.*
449 *Infect. Dis.* **65**, 1–5 (2017).
- 450 33. Junglas, B. *et al.* *Ignicoccus hospitalis* and *Nanoarchaeum equitans*: ultrastructure,
451 cell–cell interaction, and 3D reconstruction from serial sections of freeze-substituted
452 cells and by electron cryotomography. *Arch. Microbiol.* **190**, 395 (2008).
- 453 34. Anantharaman, K. *et al.* Analysis of five complete genome sequences for members
454 of the class Peribacteria in the recently recognized Peregrinibacteria bacterial
455 phylum. *PeerJ* **4**, e1607 (2016).
- 456 35. Kushkevych, I., Coufalová, M., Vítězová, M. & Rittmann, S. K.-M. R. Sulfate-
457 Reducing Bacteria of the Oral Cavity and Their Relation with Periodontitis—Recent
458 Advances. *J. Clin. Med.* **9**, 2347 (2020).

459 36. McCliment, E. A. *et al.* Colonization of nascent, deep-sea hydrothermal vents by a
460 novel Archaeal and Nanoarchaeal assemblage. *Environ. Microbiol.* **8**, 114–125
461 (2006).

462
463
464
465
466
467
468
469
470
471
472
473
474
475
476
477
478
479
480
481
482
483
484
485
486

487 **RESEARCH IN CONTEXT**

488 **Evidence before this study**

489 There is non evidence regarding the presence of the Nanoarchaea in human. The
490 previous study had shown that Nanoarchaea are present in environmental biota
491 specially in hypersaline lac.

492 **Added value of this study**

493 This study is the first to have initiated the detection of Nanoarchaea by molecular
494 approaches and by culture-based technics in human microbiota and this is the first to
495 have showed that human oral microbiota is colonized by viable Nanoarchaea which is
496 *Nanopusillus massiliensis*.

497 **Implications of all the available evidence**

498 In this study, using specific laboratory tools oriented towards the detection of
499 Nanoarchaea comprising of microscopic observations, molecular investigations
500 culminating in one whole genome sequence and isolation in coculture, we discovered
501 an unprecedented Nanoarchaea species *Nanopusillus massiliensis* detected and
502 isolated in dental plate samples which showed a close physical contact with
503 *Methanobrevibacter oralis*. This discovery extends our knowledge on the diversity of the
504 human microbiota and open a new field of research which is the Nanoarchaea in clinical
505 microbiology.

506

507

508

509

510 **Acknowledgements.** The authors thank all Hitachi team members in Japan for the
511 collaborative study with Hitachi High Technology and Institut Hospitalier Universitaire
512 and for the installation of and service of the TM4000 microscope in our facility.

513 We thank Mr Louis TSAKOU NGOUAFO for his help in *Nanopusilus Massiliensis*
514 genome finishing and Mrs. Sarah BELLALI for her help in microscopy analysis.

515 **FUNDING**

516 YS benefits from PhD grants from the Fondation Méditerranée Infection, Marseille,
517 France. This work was supported by the French Government under the
518 «Investissements d'avenir» (Investments for the Future) program managed by the
519 Agence Nationale de la Recherche (ANR, fr: National Agency for Research), (reference:
520 Méditerranée Infection 10- IAHU-03).

521

522 **COMPETING INTEREST STATEMENT**

523 All the authors declare that there are no conflicts of interest.

524

525

526

527

528

529

530

531

532 **Figures**

533 **Figure 1.** a-b, Fluorescent in situ hybridization representative detection of *Nanopusillus*
534 *massiliensis* and *Methanobrevibacter oralis* in dental plaque. (A) overlay of universal
535 DNA DAPI staining exhibiting blue microorganisms, red ARC 915 and green
536 nanoarchaeota 515mcR2 probes exhibiting organisms with the coccis form stuck to the
537 surface of a methanogen . Scale bar, 10 μ m. c-d, nanoarchaeota in dental plaque were
538 observed using scanning electron microscopy with TM4000PLus (Hitachi).e, Rhizome
539 representation of *Candidatus Nanopusillus massiliensis* based on the protein
540 sequences. The best hit for each coding gene was chosen following a comparison using
541 BLASTp, according to the following criteria: minimum of identity: 30% minimum of
542 coverage: 40% and maximum evalue: 0.001. The presentation of rhizome was built
543 using Power BI software. f, OrthoANI heatmaps between *Nanopusillus massiliensis* and
544 other Nanoarchaea genomes. OrthoANI matrix was visualized using MORPHEUS
545 software (<https://software.broadinstitute.org/morpheus/>).

546 **Figure 2.** Genome sequence-derived metabolic pathways of the clinical nanoarchaea
547 *Nanopusillus massiliensis*.

548 **Figure 3.** Tracking of the culture by scanning electron microscopy (SU5000). A. culture
549 pellet before deglycosylation. B. culture pellet After deglycosylation. C-H deglycosylated
550 pellet inoculum: culture at D15. k-o deglycosylated pellet inoculum: culture at D30. B
551 Tracking of the culture by fluorescence *in situ* hybridization. a-b deglycosylated pellet
552 inoculum: culture at D30.

553

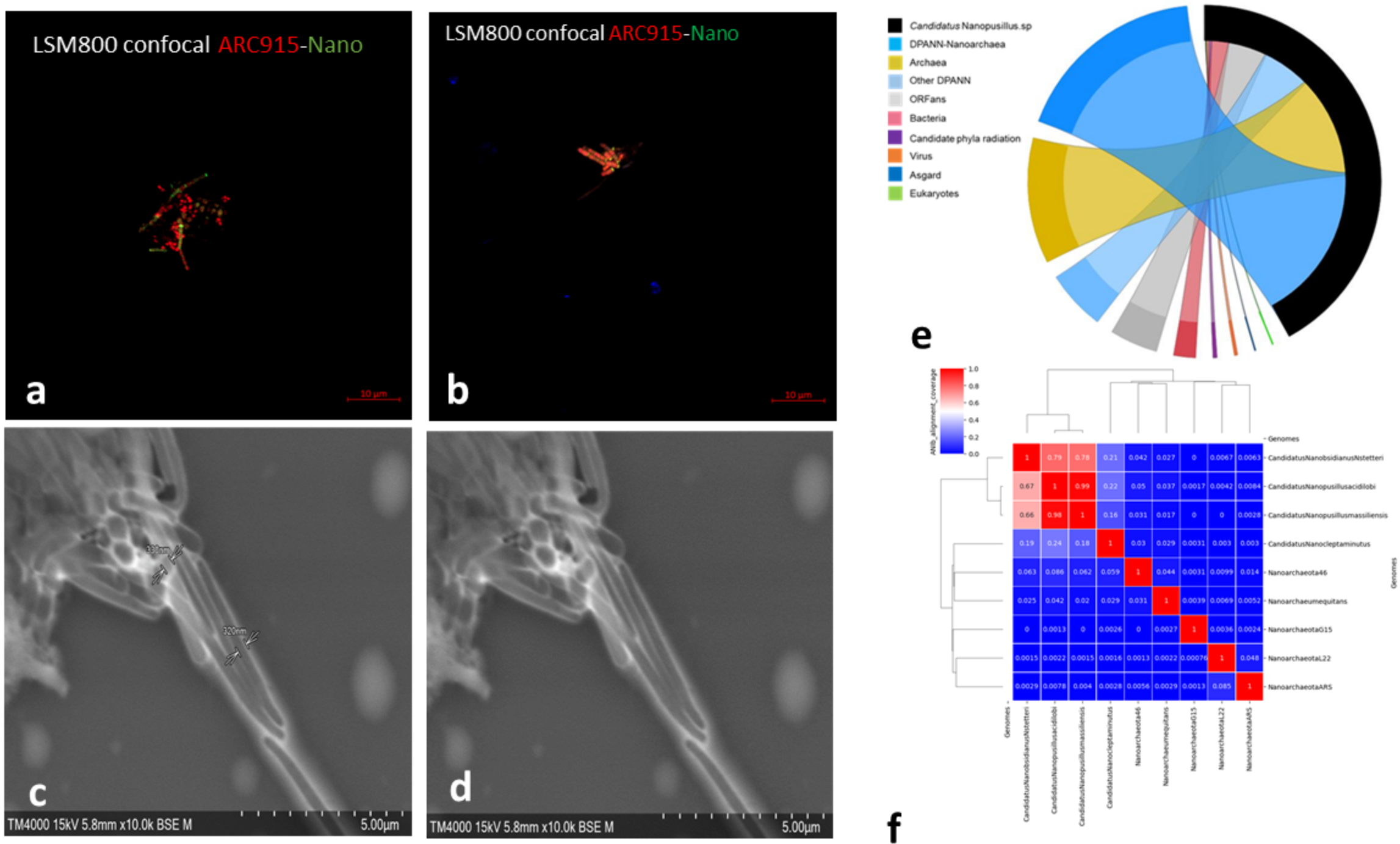


Figure 1. a-b, Fluorescent *in situ* hybridization representative detection of *Nanopusillus massiliensis* and *Methanobrevibacter oralis* in dental plaque. (A) overlay of universal DNA DAPI staining exhibiting blue microorganisms, red ARC 915 and green nanoarchaeota 515mcR2 probes exhibiting organisms with the coccis form stuck to the surface of a methanogen . Scale bar, 10 µm. c-d, nanoarchaeota in dental plaque were observed using scanning electron microscopy with TM4000Plus (Hitachi).e, Rhizome representation of *Candidatus Nanopusillus massiliensis* based on the protein sequences. The best hit for each coding gene was chosen following a comparison using BLASTp, according to the following criteria: minimum of identity: 30% minimum of coverage: 40% and maximum evalule: 0.001. The presentation of rhizome was built using Power BI software. f, OrthoANI heatmaps between *Nanopusillus massiliensis* and other Nanoarchaea genomes. OrthoANI matrix was visualized using MORPHEUS software (<https://software.broadinstitute.org/morpheus/>)

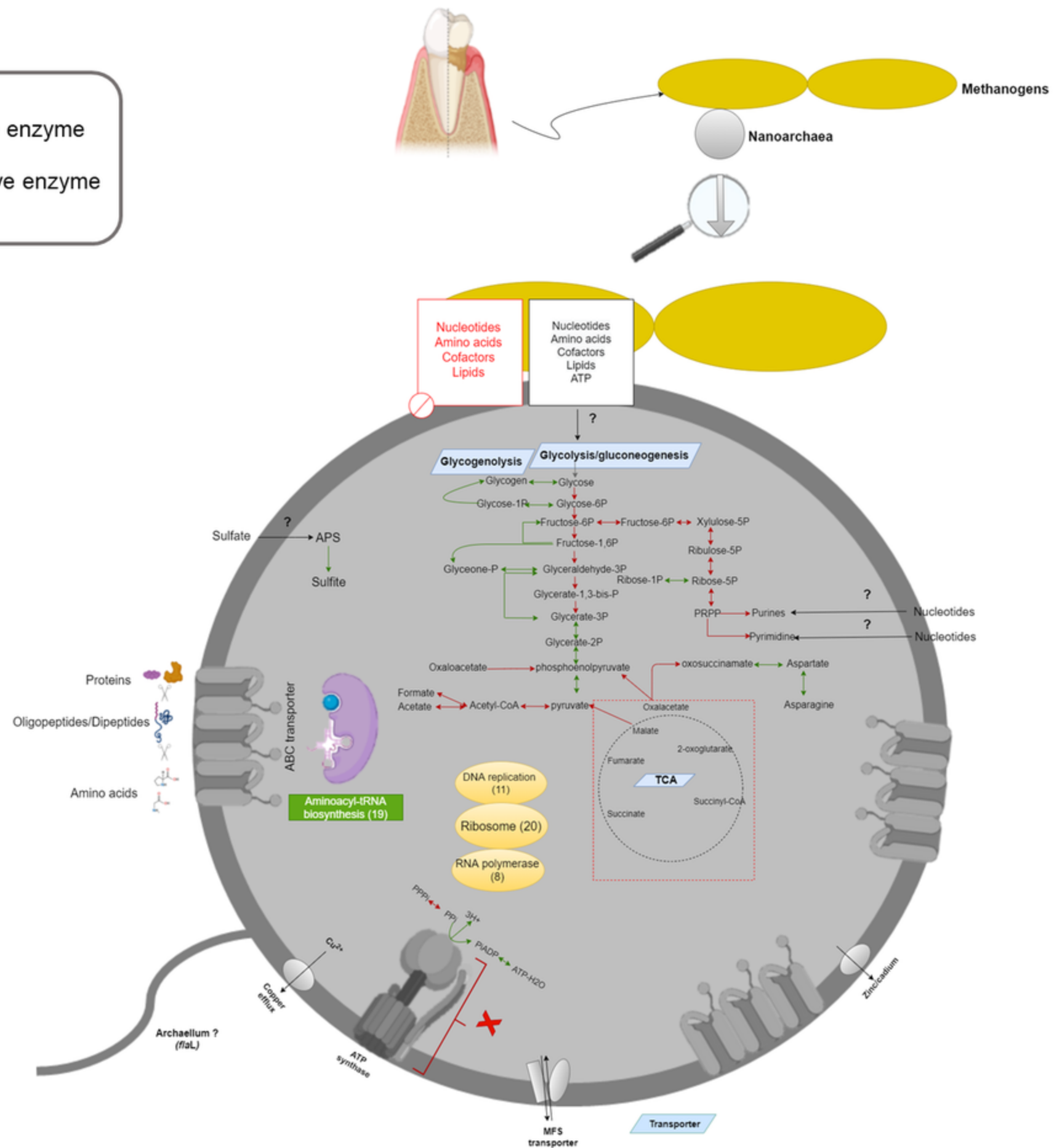


Figure 2. Genome sequence-derived metabolic pathways of the clinical nanoarchaea *Nanopusillus masliensis*.

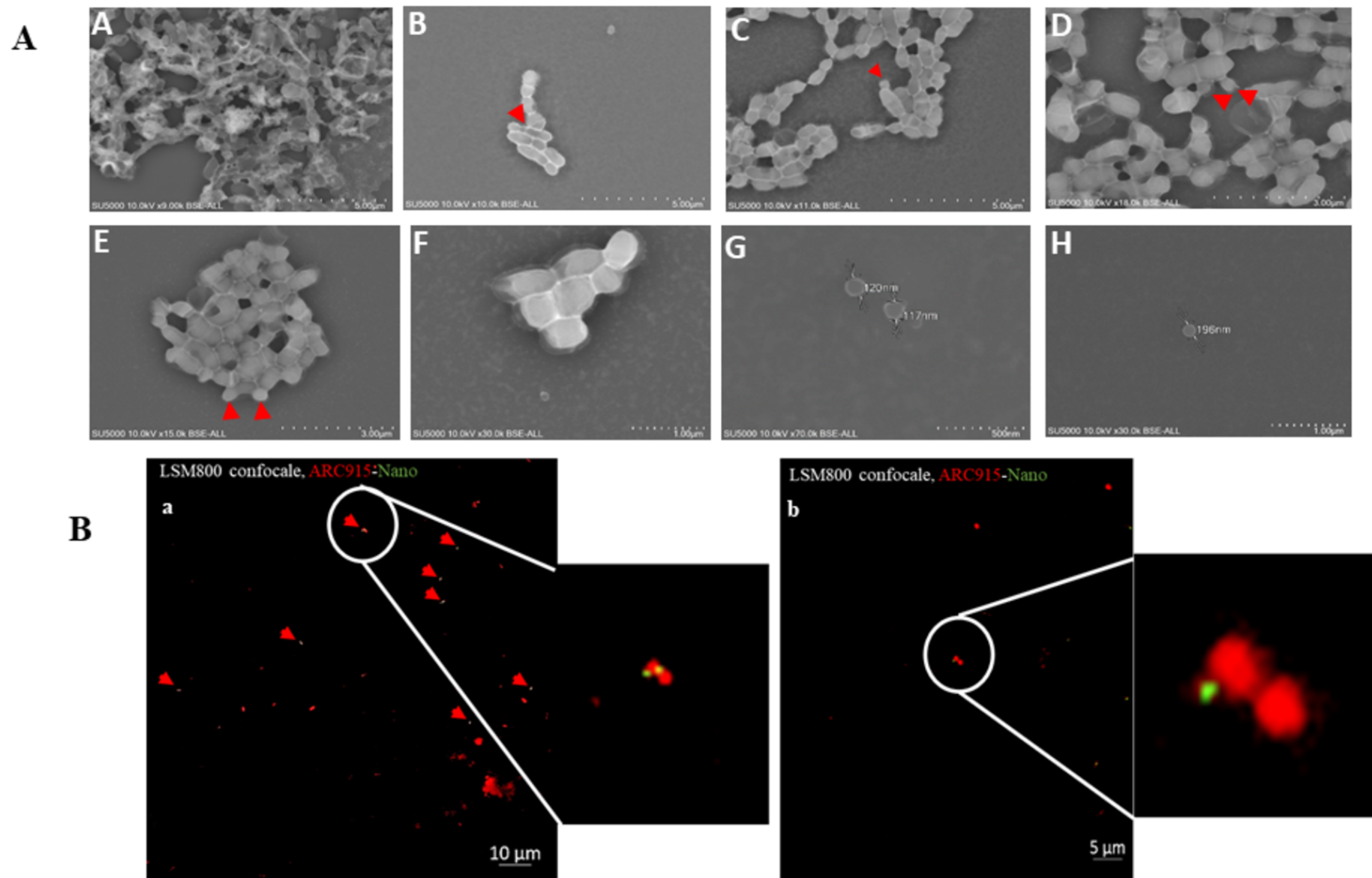


Fig3. **A** Tracking of the culture by scanning electron microscopy (SU5000). **A.** culture pellet before deglycosylation. **B.** culture pellet After deglycosylation. **C-H** deglycosylated pellet inoculum: culture at D15. **B** Tracking of the culture by fluorescence *in situ* hybridization. **a-b** deglycosylated pellet inoculum: culture at D30.